EPJ Web of Conferences **309**, 04015 (2024) https://doi.org/10.1051/epjconf/202430904015
EOSAM 2024

Optimizing Plasmonic Microarray Biosensors: Custom Optical System for Enhanced Evaluation and Characterization

Lóránt Tibor Csőke[1,3,*], *Andrea* Csáki[2,**], and *Zsolt* Kollár[3,***]

[1]Optimal Optik Ltd., Dayka Gábor u. 6/b, 1118 Budapest, Hungary
[2]Leibniz Institute of Photonic Technology, (Leibniz-IPHT) Department Nanobiophotonics A.-Einstein-Str. 9, 07745 Jena, Germany
[3]Budapest University of Technology and Economics, XI. Magyar tudósok körútja 2. I ép. E szárny, H-1117 Budapest, Hungary

Abstract. This paper presents the design and implementation of a tailored optical system for rapid characterization of transmission-based localized surface plasmon resonance (LSPR) biosensors. The system incorporates a motorized monochromator, offering extreme versatility in experimenting with wavelength resolution and bandwidth of the illumination. This setup streamlines the process of determining optimal chip design parameters such as the density of nanoparticles and the number of detection wavelengths required, as measurements are fully automated and software-driven. Furthermore, the system facilitates straightforward detection of manufacturing errors, including misaligned spots or inhomogeneous particle distribution, enhancing overall efficiency and reliability in biosensor evaluation.

1 Introduction

Localized surface plasmon resonance (LSPR) sensors have emerged as a powerful tool for various applications, including medical diagnosis, environmental monitoring, and disease detection [1]. The predominant approach in LSPR sensing involves examining the extinction spectra of nanoparticle ensembles localized on a transmissive substrate, typically accomplished through spectrometry or hyperspectral imaging [2]. Minute alterations in the refractive index surrounding the nanoparticles induce a shift in their resonance wavelength [2]. For field instruments, the number of detection wavelengths the optical system is designed for significantly impacts cost. Hence, determining the optimal wavelength resolution constitutes a primary focus of current research. A secondary yet critical consideration is the nanoparticle density. Depending on the particle spacing, near-field enhancement can further improve the sensitivity of the sensor [3]. The main goal of this research is to address these factors and find an optimum for both parameters by the design and construction of a high end laboratory optical setup. This study centers on a particular type of microfluidic LSPR sensor developed and produced by Csáki et al. at Leibnitz IPHT (Jena, Germany) [4]. The paper is structured as follows: Section 2 delineates the fundamental methodology for performing readouts with this specific microfluidic LSPR sensor. Section 3 presents the laboratory setup constructed for this purpose and highlights its primary features. Finally, Section 4 provides a summary of the evaluation findings, followed by conclusions drawn from the study.

*e-mail: csoke.lorant@edu.bme.hu
**e-mail: andrea.csaki@leibniz-ipht.de
***e-mail: kollarzs@mit.bme.hu

2 Readout strategy of microfluidic LSPR array sensors

These sensors are fabricated by depositing a concentrated colloid solution of gold nanoparticles onto glass coverslips using a piezoelectric dispenser, as detailed in [4]. Subsequently, the coverslips containing the dried and immobilized spots are integrated into pre-machined microfluidic chamber crafted from a transmissive material [4]. The measurement setup is straightforward: the sample is illuminated from its backside with a specific wavelength, while transmission images are captured using a monochrome camera. By incrementally varying the wavelength and capturing an image for each step, a hyperspectral database can be constructed.

3 Proposed optical system for enhanced readout

The presented fully automated system aims to expedite the evaluation of these sensors, thereby improving the development and optimization process of LSPR devices. It incorporates a high-power white light module, driven by a laser. This module is linked to a motorized monochromator (Optics Focus - 7IMS3011B) via an optical fiber (D = 1 mm, 0.5 NA). The monochromator's output is connected to an optical fiber the same type as for the light source, which ends in a 2-axis actuator. The fiber's end is magnified by a factor of 5 and projected onto the LSPR sensor via an achromatic lens. To ensure consistent acquisition and evaluation, a coupler is integrated into the beam path to allow simultaneous measurement of the illumination spectra, thus enabling the detection of any potential wavelength shifts. The image of the back-illuminated

chip is captured by a monochrome camera (Contrastech Mars 3800-10gm) equipped with a telecentric lens (Edmund Optics - 88348).

4 Experimental section and results

In this study, we investigated a particular type of LSPR array sensor known as a gradient chip. This chip features distinct lines of spots, each characterized by varying nanoparticle density, enabling the assessment of interparticle distance effects. Images were captured at various wavelengths ranging from 500 nm to 700 nm, with increments of 10 nm and a bandwidth of 6 nm. The images were first segmented to identify and isolate the plasmonic array spots from the background. Absorbance values are derived based on the ratio between the intensity of the surrounding background on the image and the segmented spot. In our current experimental setup, we prepared four sucrose solutions with increasing concentration, determined using a handheld refractometer (Labornite RHW-25Brix ATC). The sugar concentration, measured in Brix, was then utilized to calculate the refractive index of each solution using the ICUMSA table [5]. By evaluating the centroid shifts in both wavelength and absorbance dimensions of the extinction spectra, we determined the refractive index sensitivity of individual spots. Plotting these sensitivity values against the particle density of spots allows us to easily identify the optimal concentration, as depicted in Figure 1.

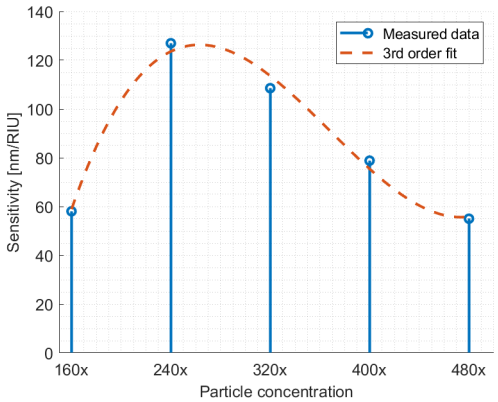

Figure 1. Averaged sensitivity over the same density spots for each concentration

A secondary experiment was conducted to explore the impact of wavelength resolution. When the number of wavelengths used for measuring the extinction spectra is reduced, the accuracy of peak shift detection diminishes. A threshold can be established, beyond which further reduction in the number of detection wavelengths would compromise the consistent determination of centroid wavelength shift. Fig. 2 illustrates the sum of absolute errors of peak wavelength shifts for each refractive index step between the original ($\Delta\lambda = 10\ nm$) sampling and the sparse samplings. In Fig. 2, the actual wavelength shift for the highlighted refractive index change, determined from the high-density sampling, is depicted as a horizontal dashed line. It's evident that further reduction in the number of wavelengths results in higher errors compared to the peak shift itself, making evaluation impractical.

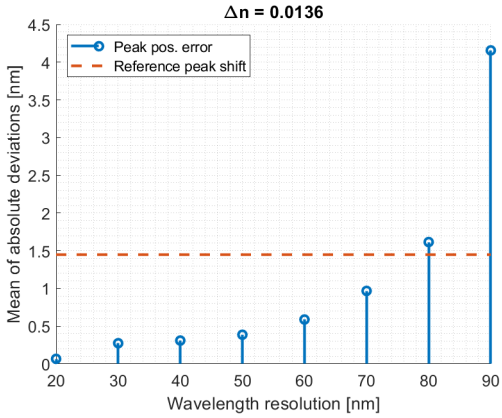

Figure 2. Calculated deviations from the reference data

5 Conclusions

In this study, we developed a highly automated evaluation platform aimed at optimizing LSPR sensor manufacturing processes. Leveraging this laboratory setup, we were able to deduce optimal particle concentrations and determine the required number of detection wavelengths for a specific type of LSPR sensor. The system demonstrates remarkable efficiency, capable of measuring the transmission spectra of spotted gold nanoparticle ensembles in less than 60 seconds, spanning a wavelength range from 500 to 700nm. Moreover, our setup validated its efficacy by accurately determining LSPR sensitivity values within the range of 100-130nm/RIU, as reported in existing literature. Moving forward, we plan to extend our investigations to include additional sensor types and explore various chip synthesis parameters.

References

[1] A. Bonyár, ACS Applied Nano Materials **3**, 8506 (2020)

[2] D. Zopf, J. Jatschka, A. Dathe, N. Jahr, W. Fritzsche, O. Stranik, Biosensors and Bioelectronics **81**, 287 (2016)

[3] T. Lednický, A. Bonyár, ACS Applied Materials & Interfaces **12**, 4804 (2020)

[4] D. Zopf, A. Pittner, A. Dathe, N. Grosse, A. Csáki, K. Arstila, J.J. Toppari, W. Schott, D. Dontsov, G. Uhlrich et al., ACS Sensors **4**, 335 (2019)

[5] International Commission for Uniform Methods of Sugar Analysis, *Icumsa specifications and standards* (2022), accessed: 2024-05-17, `https://www.icumsa.org/sps`